BB

GANIL

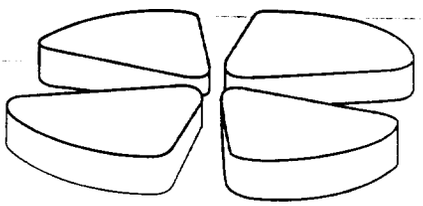

Mass Measurement of ^{100}Sn

M. Chartier[1)], G. Auger[1)], W. Mittig[1)], A. Lépine–Szily[2)], L.K. Fifield[3)], J.M. Casandjian[1)], M. Chabert[1)], J. Fermé[1)], A. Gillibert[4)], M. Lewitowicz[1)], M. Mac Cormick[1)], M.H. Moscatello[1)], O.H. Odland[5)], N.A. Orr[6)], G. Politi[7)], C. Spitaels[1)], A.C.C. Villari[1)]

1. GANIL, Bld Henri Becquerel, BP 5027, 14021 Caen Cedex, France
2. IFUSP-Universidade de São Paulo, C.P.66318, 05389-970 São Paulo, Brasil
3. Dep. of Nuclear Physics, RSPhySE, Australian National University, ACT 0200, Australia
4. CEA/DSM/DAPNIA/SPhN, CEN Saclay, 91191 Gif-sur-Yvette, France
5. Universitetet i Bergen, Fysisk Institutt, Allégaten 55, 5007 Bergen, Norway
6. LPC-ISMRA, Bld du Maréchal Juin, 14050 Caen Cedex, France
7. Universitá di Catania, Dip. di Fisica, Corso Italia 57, 95125 Catania, Italy

Submitted to Physical Review Letters

GANIL P 96 12

SW9622

Mass Measurement of ^{100}Sn

M. Chartier[1], G. Auger[1], W. Mittig[1], A. Lépine–Szily[2], L.K. Fifield[3], J.M. Casandjian[1], M. Chabert[1], J. Fermé[1], A. Gillibert[4], M. Lewitowicz[1], M. Mac Cormick[1], M.H. Moscatello[1], O.H. Odland[5], N.A. Orr[6], G. Politi[7], C. Spitaels[1], A.C.C. Villari[1]

1. GANIL, Bld Henri Becquerel, BP 5027, 14021 Caen Cedex, France
2. IFUSP-Universidade de São Paulo, C.P.66318, 05389-970 São Paulo, Brasil
3. Dep. of Nuclear Physics, RSPhySE, Australian National University, ACT 0200, Australia
4. CEA/DSM/DAPNIA/SPhN, CEN Saclay, 91191 Gif-sur-Yvette, France
5. Universitetet i Bergen, Fysisk Institutt, Allégaten 55, 5007 Bergen, Norway
6. LPC-ISMRA, Bld du Maréchal Juin, 14050 Caen Cedex, France
7. Universitá di Catania, Dip. di Fisica, Corso Italia 57, 95125 Catania, Italy

April 26, 1996

Abstract

Secondary ions of ^{100}Ag, ^{100}Cd, ^{100}In and ^{100}Sn were produced via the fusion-evaporation reaction ^{50}Cr + ^{58}Ni at an energy of 5.1 MeV/nucleon, and were accelerated simultaneously in the second cyclotron of GANIL (CSS2). About 10 counts were observed from the production and acceleration of ^{100}Sn^{22+}. The masses of ^{100}Cd, ^{100}In and ^{100}Sn were measured with respect to ^{100}Ag using the CSS2 cyclotron, with precisions of 2×10^{-6}, 3×10^{-6} and 10^{-5} respectively.

PACS numbers : 21.10.Dr, 27.60.+j

The doubly-magic nucleus ^{100}Sn was recently produced and identified in two independent experiments using the projectile fragmentation technique : at GSI with a 1.1 GeV/nucleon ^{124}Xe beam [1] and at GANIL using a 63 MeV/nucleon ^{112}Sn beam [2]. Due to its N = Z character at the double shell closure, it has been keenly sought, and its observation represents the culmination of many years of effort. However, its observation demonstrates only that it is bound against proton decay whereas a measurement of its mass provides more detailed information on the interaction between protons and neutrons in the same high lying shell model orbits and shell closure near the proton drip-line.
The method available for measuring masses of nuclei produced in fragmentation reactions employs time-of-flight over a linear flight path of $\sim 50 - 100$ m [3, 4, 5, 6, 7, 8] , using high precision magnetic spectrometers (SPEG [9] at GANIL and TOFI [10] at Los Alamos). With currently available count rates, the resolution of these devices is not good enough to perform precise mass measurement of ^{100}Sn. Given the much increased path length when the ions follow a spiral trajectory, we have developed a method using the second cyclotron of GANIL (CSS2) as a high precision spectrometer. The mass resolution obtained with the simultaneous acceleration of A/q = 3 light ions (^{6}He, ^{9}Li) was shown to be 10^{-6} [11, 12].

In the present work, ^{100}Sn nuclei, together with nuclei of ^{100}Ag, ^{100}Cd and ^{100}In were produced by a fusion-evaporation reaction and accelerated simultaneously. The mass resolution achieved with these heavy ions was of the order of 3×10^{-5}. Using the mass of ^{100}Ag as a

reference, the masses of ^{100}Cd, ^{100}In and ^{100}Sn could be determined with precisions (depending on the statistics) of 2×10^{-6}, 3×10^{-6} and 10^{-5} respectively.

Details of the method used with light ions have already been published [12], so here we will concentrate on features specific to the present work. The method consists in substituting the existing stripper located between the two cyclotrons by a production target, in which the secondary nuclei are produced and are subsequently injected into and accelerated by CSS2. Figure 1 shows a schematic diagram of the experimental set-up.

Neutron-deficient A = 100 nuclei were produced by fusion-evaporation reactions between a $^{50}Cr^{9+}$ beam accelerated by the CSS1 cyclotron and a ^{58}Ni target. This reaction is known to be very favourable for the production of nuclei around ^{100}Sn [13]. The highest cross-section is for the production of ^{100}Ag, followed by ^{100}Cd and ^{100}In. Using the Monte-Carlo codes PACE and HIVAP, the optimal energy for the production of ^{100}Sn was estimated to be 255 MeV.

Considerations of matching between the two cyclotrons further require that the ratio of the velocities v_1 and v_2 at extraction from CSS1 and at injection into CSS2 respectively should satisfy :

$$\frac{v_2}{v_1} = \frac{2}{h_2} \tag{1}$$

where h_2 is the CSS2 harmonic (number of Radio-Frequency periods per turn). Since the velocity of the compound system is somewhat less than 0.5 v_1, the lowest practicable harmonic is $h_2 = 5$. The incident beam energy of 265 MeV and the target thickness of 1.3 mg/cm^2 were therefore chosen to maximise the yield of ^{100}Sn nuclei emerging from the target with $v_2 = 2/5\ v_1$. In order to allow the use of beam currents between 300 and 500 nAe, the target was rotated and cooled.

Accelerated ions were detected inside the cyclotron using a silicon detector telescope (ΔE 35μm, E 300μm) mounted on a radial probe which can be moved from the injection radius (1250 mm) up to the extraction radius (3000 mm). The time-of-flight, or phase (one RF period being equal to 360^o), of the detected ions was measured relative to the RF signal of the CSS2 cyclotron. For two nuclei, masses m and $m + \delta m$, accelerated simultaneously in CSS2, the separation in time, δt, after N_T turns is given to first order by :

$$\frac{\delta t}{t} = \frac{\delta m}{m} \tag{2}$$

where t is the total transit time, $t = N_T.h_2/f$, and f is the frequency of the accelerating voltage.This relation is the basis of the calibration procedure : the unknown mass $m + \delta m$ can be determined from the well known reference mass m if the number of turns N_T or the total time-of-flight t are known.

Since the most probable charge state of the A = 100 secondary ions emerging from the target was 22^+, it was possible to use $^{50}Cr^{11+}$ to tune the cyclotron. These ions were produced by degrading the primary ^{50}Cr beam to 2/5 of its initial velocity in a 22 mg/cm^2 Ta target. Their intensity was not, however, sufficient to tune the cyclotron in the standard way using the measurement of currents, and thus it was necessary to use the silicon detector telescope also to map the phase as a function of radius during the tuning procedure. Once isochronism, as indicated by constant phase with increasing radius and complete separation of individual orbits [14], had been established, the target was changed to ^{58}Ni and the cyclotron's magnetic field

was increased by $\delta B/B = 4.7 \times 10^{-4}$. This equals the estimated fractional difference in the mass/charge ratio between $^{50}Cr^{11+}$ and $^{100}Sn^{22+}$ [15]. Hence, at this new field, $^{100}Sn^{22+}$ ions would have been accelerated with the same phase and isochronism curve as achieved for $^{50}Cr^{11+}$ at the end of the tuning process. The cyclotron acceptance for the simultaneous acceleration of different ions is between $10^{-2} - 10^{-4}$, strongly dependent on target homogeneity and the specific reaction considered. The predicted fractional mass/charge difference between $^{100}Sn^{22+}$ and $^{100}Ag^{22+}$ [15] is 2.3×10^{-4}, whence it is possible to accelerate $^{100}Ag^{22+}$, $^{100}Cd^{22+}$, $^{100}In^{22+}$ and $^{100}Sn^{22+}$ simultaneously to maximum radius in CSS2 [12]. However, with increasing radius, the phase of ions other than $^{100}Sn^{22+}$ moves further and further ahead of the isochronous phase.

Figure 2 (a) shows a plot of total energy versus phase for ions with A = 100 and q = 22^+ detected in the silicon detector telescope near maximum radius in CSS2. This spectrum is a composite of a series of spectra acquired with the radial probe at radii between 2935 mm and 2995 mm. Note that the increasing phase corresponds to smaller time-of-flight and thus to smaller mass. To aid the interpretation of this spectrum, a simulation of the ion trajectories in the cyclotron has been performed, and is shown in Figure 2 (b). This simulation incorporates the observation that the tuning with $^{50}Cr^{11+}$ resulted in a phase of -10° close to the extraction radius. Thus $^{100}Sn^{22+}$ is expected around -10° and lighter nuclei are detected at larger phases, proportional to their fractional mass/charge differences. For the $^{100}Ag^{22+}$ ions, which are furthest from isochronism, portions of several turns are intercepted by the detector at a given radius. For ions closer to isochronism, the spread in energies or radii for a single turn are less and fewer turns are intercepted at a fixed radius. These features are clearly visible in Figure 2 (a). Several turns of the prolifically produced ^{100}Ag ions may be seen, and ^{100}Cd are also evident. The intensities of ^{100}In and ^{100}Sn ions are not high enough for them to be readily apparent in this plot. There is a cluster of events with the correct energies and phases to be ^{100}Sn ions, but there is also a comparable number of background events with the correct phase but lower energies. These background events could be attributed mainly to a tail of ^{100}Ag.
In order to separate genuine ^{100}Sn events from background, a particle identification parameter $f(Z)$, proportional to the atomic number Z, was derived from a linear combination of the signals from the two detectors of the silicon detector telescope. The coefficients were determined empirically from the data by varying the total energy of the products detected in the silicon detector telescope (related to the radial position of the probe). Figure 3 shows a plot of this identification parameter versus phase. The horizontal lines mark off the regions where the bulk of each ion species is to be found. Note that, in the region of phase around -10° where the ^{100}Sn events are expected, there is a scattered background of events in the Ag and Cd windows, very few in the In window, and several events in the Sn window. This can be seen more clearly in Figure 4 which shows total energy versus phase plots for events falling within the In and Sn windows of Figure 3, and their projections on to the phase axis. There is an excess of 10-12 events in the Sn spectra of Figure 4 around -10° which have correct phase, total energy and $f(Z)$ value simultaneously, and these are attributed to $^{100}Sn^{22+}$ ions. Note that the bulk of the events in both the In and Sn spectra are due to tails of the much more intense ^{100}Ag and ^{100}Cd groups. The relative intensities of these Ag and Cd events in the In and Sn spectra respectively differ by a factor of ten. If it is assumed that the background near -10° is due to Ag and Cd ions, then this background would be expected to scale accordingly. Since there are only 4 background counts in the In spectrum, the expected background in the Sn spectrum is therefore no more than 1 count.

In order to determine the masses of the various isobars it is necessary to determine their centroids in phase. This was accomplished using an iterative procedure to subtract the Ag

contribution from the Cd spectrum, the Ag and Cd contributions from the In spectrum, and the Ag, Cd and In contributions from the Sn spectrum to arrive at fairly pure spectra (in the anticipated region of phase) for each of the four isobars, from which the centroids could be determined. The number of turns before detection, N_T, which was required to turn the time differences between the various isobars and ^{100}Ag into mass differences, according to equation 2, was determined in a separate measurement at the conclusion of the experiment. Finally, we arrive at the following mass excesses :

$$M.E.(^{100}Cd) = -74.180 \pm 0.200(syst.)MeV$$

$$M.E.(^{100}In) = -64.650 \pm 0.300(syst.) \pm 0.100(stat.)MeV$$

$$M.E.(^{100}Sn) = -57.770 \pm 0.300(syst.) \pm 0.900(stat.)MeV$$

The systematic uncertainties take account of the uncertainties in the subtraction procedure described above. We supposed that there were no long-lived isomeric states. These masses are to be compared with the experimental values presented in the Audi-Wapstra mass table [15] for ^{100}Cd (-74.310 ± 0.100 MeV) [16] and also for ^{100}In (-64.130 ± 0.380 MeV) which was obtained from the combination of an indirect measurement [17] and our previous direct measurement using the CSS2 cyclotron technique [18]. The mass of ^{100}Sn (-56.860 ± 0.430 MeV) given in the Audi-Wapstra mass table [15] is an estimate based on extrapolating systematic trends. Our mass of ^{100}Cd is in good agreement with the existing measurement, which gives good confidence in the new results for ^{100}In and ^{100}Sn.

It is of interest to compare our experimental count rates to statistical model calculations. As noted above, the absolute transmission of the CSS2 is difficult to determine. However, if we suppose that the mean charge distribution for the different isobars is centered approximately at the same value (which could be wrong, e.g. if delayed Auger electron emission changed strongly the charge state after the target), we can obtain relative cross-sections. To our knowledge, only one value has been measured [19] for ^{100}Ag, which is 3.9 mb. This value is one order of magnitude lower than estimations from statistical model calculations that we used previously to estimate the absolute cross-section. If we normalize our count rates to this experimental value [19] for ^{100}Ag, we obtain the cross-sections of Table 1, all of which are an order of magnitude lower than the statistical model predictions. Note that the small 40 nb cross-section for ^{100}Sn is nonetheless three orders of magnitude larger than the ones in fragmentation reactions [1, 2].

We compared the shell model calculations of Johnstone and Skouras [20] to the Audi-Wapstra mass table [15] for the binding energies of isotones N = 50, 51 and 52 (see Figure 5). We can see that the calculations and the values of the table are in good agreement as far as experimental data are available (up to ^{98}Ag and ^{100}Cd). But there is a clear disagreement when the mass table values are derived by extrapolating systematic trends. On Figure 5 are represented 33 nuclei from ^{90}Zr to ^{102}Sn. We added on the same graph our experimental results for ^{100}Cd, ^{100}In and ^{100}Sn (represented by black stars). As is visible, the shell model calculations agree well with our results, predicting a stronger binding energy than the extrapolations from systematics. At the moment, it is difficult to determine the possible origin of this overbinding. For lighter N = Z nuclei, a strong overbinding is observed and can be attributed to a Wigner term. In a recent work [21], it was shown that this term corresponds to a SU(4) symmetry. It is expected that this term will decrease due to SU(4) symmetry breaking by Coulomb interaction and high angular momenta. It decreases from about 4 MeV around Z = 8, to 1.7 MeV in ^{56}Ni. It is an interesting question up to which mass number A this symmetry persists. We hope that the present data and other data on mid-shell nuclei presently being analysed will contribute to

answer this question. Calculations over a larger domain around N = Z = 50 would be desirable, too, in order to disentangle different effects.

In conclusion, ^{100}Sn has been observed as the product of a fusion-evaporation reaction for the first time using the CSS2 cyclotron of GANIL as an efficient high precision mass spectrometer. The masses of not only ^{100}Sn, but also ^{100}In and ^{100}Cd were determined using ^{100}Ag as a reference. The known mass excess of ^{100}Cd has been confirmed within 2×10^{-6} and we measured for the first time the masses of ^{100}In and ^{100}Sn with a precision of 3×10^{-6} and 10^{-5} respectivly. A preliminary production cross-section of 40 nb has been determined for the fusion-evaporation reaction ^{50}Cr + ^{58}Ni $\longrightarrow$ ^{100}Sn at 255 MeV.

References

[1] R. Schneider, J. Friese, J. Reinhold, K. Zeitelhack, T. Faestermann et al, Z.Phys. **A348**, 241 (1994).

[2] M. Lewitowicz, R. Anne, G. Auger, D. Bazin, C. Borcea et al, Phys.Lett. **B332**, 20 (1994).

[3] A. Gillibert, L. Bianchi, A. Cunsolo, B. Fernandez, A. Foti et al, Phys.Lett. **B176**, 317 (1986).

[4] D.J. Vieira, J.M. Wouters, K. Vaziri, R.H. Kraus Jr., H. Wollnik et al, Phys.Rev.Lett. **57**, 3253 (1986).

[5] A. Gillibert, W. Mittig, L. Bianchi, A. Cunsolo, B. Fernandez et al, Phys.Lett. **B192**, 39 (1987).

[6] J.M. Wouters, R.H. Kraus Jr., D.J. Vieira, G.W. Butler and K.E.G. Löbner, Z.Phys. **A331**, 229 (1988).

[7] X.L. Tu, X.G. Zhou, D.J. Vieira, J.M. Wouters, Z.Y. Zhou et al, Z.Phys. **A337**, 361 (1990).

[8] N.A. Orr, W. Mittig, L.K. Fifield, M. Lewitowicz, E. Plagnol et al, Phys.Lett. **B258**, 29 (1991).

[9] L. Bianchi, B. Fernandez, J. Gastebois, A. Gillibert, W. Mittig et al, Nucl.Instr.Meth. **A276**, 509 (1989).

[10] J.M. Wouters, D.J. Vieira, H. Wollnik, G.W. Butler, R.H. Kraus Jr. et al, Nucl.Instr.Meth. **B26**, 286 (1987).

[11] G. Auger, W. Mittig, A. Lépine-Szily, L.K. Fifield, M. Bajard et al, Nouvelles du GANIL **50**, 7 (1994).

[12] G. Auger, W. Mittig, A. Lépine-Szily, L.K. Fifield, M. Bajard et al, Nucl.Instr.Meth. **A350**, 235 (1994).

[13] E. Roeckl, private communication (1994).

[14] G. Auger, W. Mittig, A. Lépine-Szily, M. Chartier, D. Bibet et al, Nouvelles du GANIL **54**, 7 (1995).

[15] G. Audi and A.H. Wapstra, Nucl.Phys. **A595**, 409 (1995).

[16] K. Rykaczewski, A. Płochocki, I.S. Grant, H. Gabelmann, R. Barden et al, Z.Phys. **A332**, 275 (1989).

[17] J. Szerypo, M. Huyse, G. Reusen, P. Van Duppen, Z. Janas et al, Nucl.Phys. **A584**, 221 (1995).

[18] A. Lépine-Szily, G. Auger, W. Mittig, M. Chartier, D. Bibet et al, Proceedings of the ENAM 95 Conference on Exotic Nuclei and Atomic Masses, Arles, France, June 19-23 (1995).

[19] R. Schubart, H. Grawe, J. Heese, H. Kluge, K.H. Maier et al, Z.Phys. **A352**, 373 (1995).

[20] I.P. Johnstone and L.D. Skouras, Phys.Rev. **C51**, 2817 (1995).

[21] P. Van Isacker, D.D. Warner and D.S. Brenner, Phys.Rev.Lett. **74**, 4607 (1995).

[22] K. Rykaczewski, private communication (1995).

	Present Work		Stat. Model	Stat. Model	Stat. Model
	(c/h/nAe)	(mb)	PACE (mb)	HIVAP (mb) [13, 22]	CASCADE (mb)
^{100}Ag	~ 40	3.9 [19]	30	38	38
^{100}Cd	~ 10	~ 1	16	7	3.2
^{100}In	~ 0.01	~ 0.001	0.02	0.014	0.027
^{100}Sn	$\sim 4 \times 10^{-4}$	$\sim 4 \times 10^{-5}$	-	0.0003	-

Table 1: *Experimental cross-sections of the present work normalized to the value of Schubart et al [19] for ^{100}Ag, and compared to statistical model calculations.*

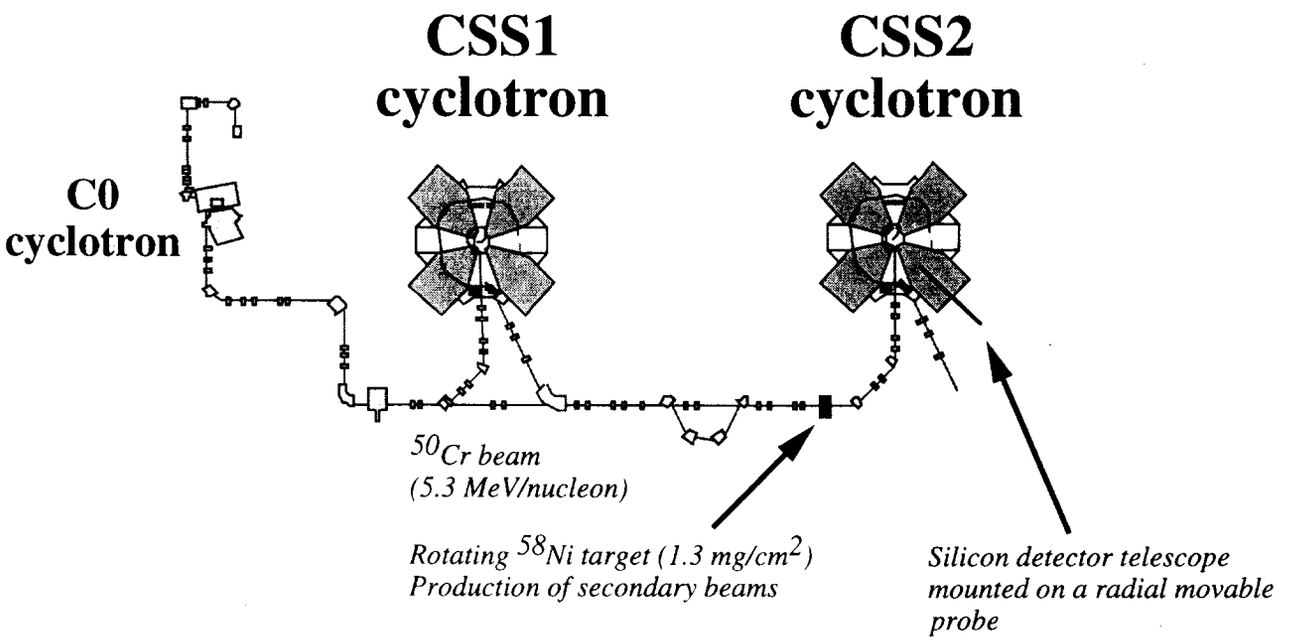

Figure 1: *Schematic diagram of the experimental set-up.*

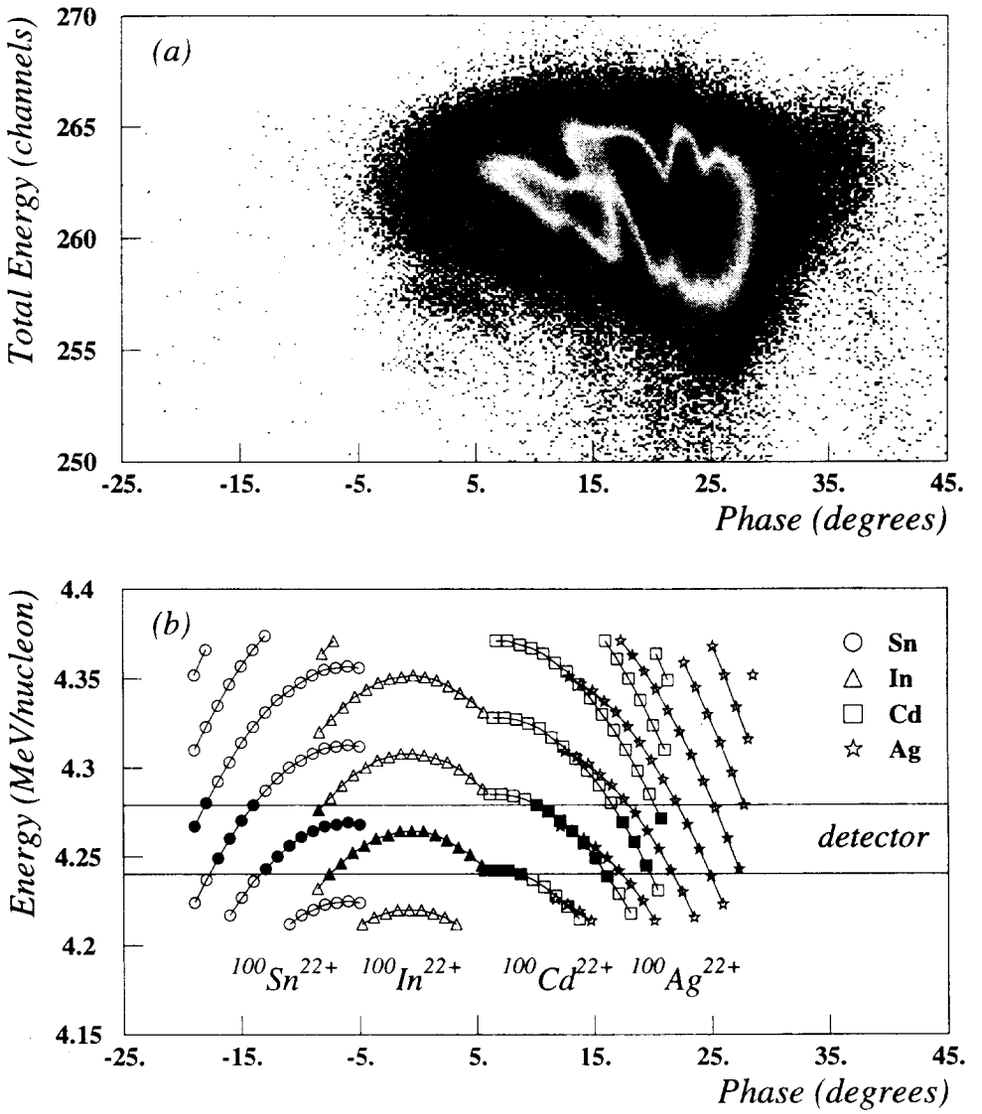

Figure 2: *Experimental and simulated energy versus phase spectra accumulated over different positions of the radial probe close to the extraction radius. (a) Experimental spectrum in which the several adjacent orbits intercepted for the most produced ions ($^{100}Ag^{22+}$ and $^{100}Cd^{22+}$) are clearly visible. A relative calibration between the energy loss in the $\Delta E(35\mu m)$ detector and the residual energy in the $E(300\mu m)$ detector allowed for the calculation of the total energy. (b) Result of a simulation for the simultaneous acceleration of $^{100}Sn^{22+}$, $^{100}In^{22+}$, $^{100}Cd^{22+}$ and $^{100}Ag^{22+}$ (without any correction for relative production rates). The cut of the detector (located at a given radius) is indicated by black symbols.*

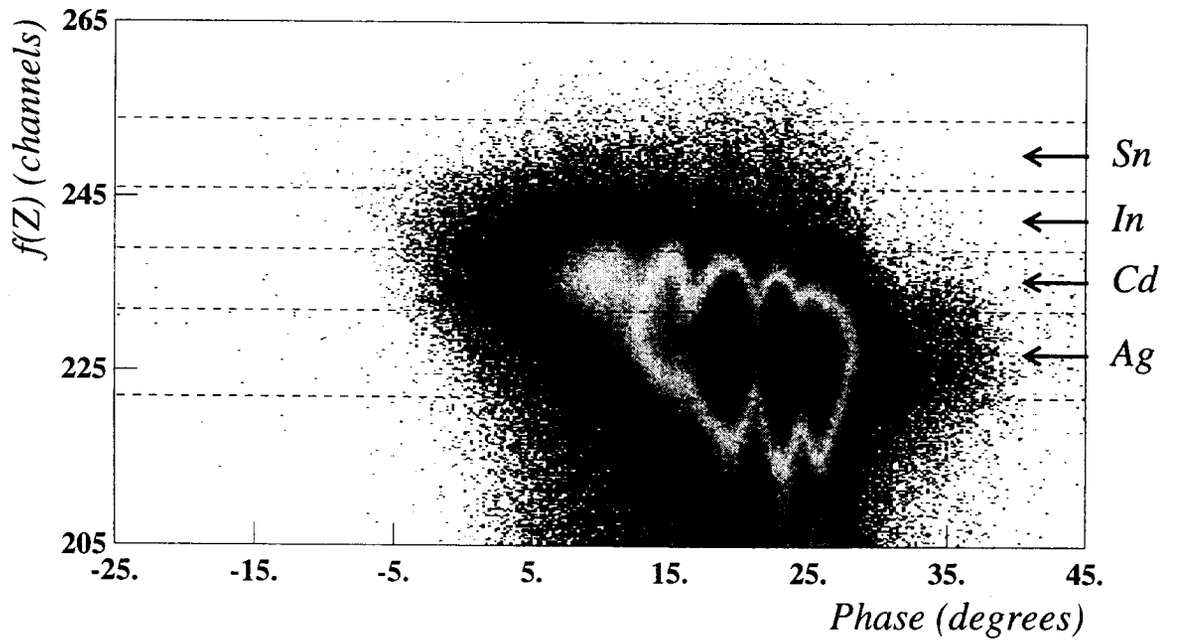

Figure 3: *Identification parameter f(Z) versus phase spectrum (see text). In this spectrum, we can set different gates corresponding to four f(Z) regions attributed to Ag, Cd, In and Sn. The big vertical tail, coming from channeling effect in the ΔE detector, has no influence on the good events.*

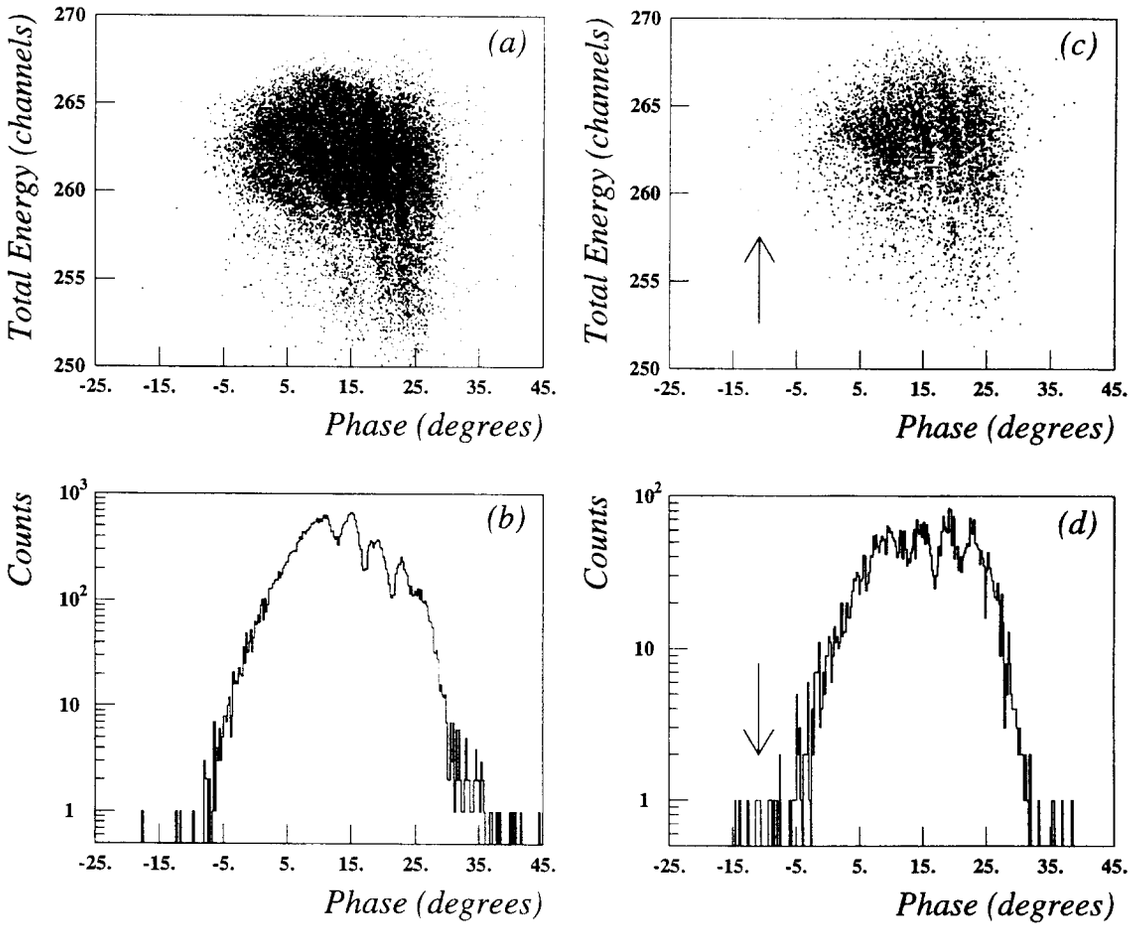

Figure 4: *Total energy versus phase spectra and their projections on to the phase axis, both gated by the identification parameter f(Z) for In [(a),(b)] and Sn [(c),(d)] respectively, as shown on Figure 3. The arrows indicate the location of* $^{100}Sn^{22+}$ *counts (see text).*

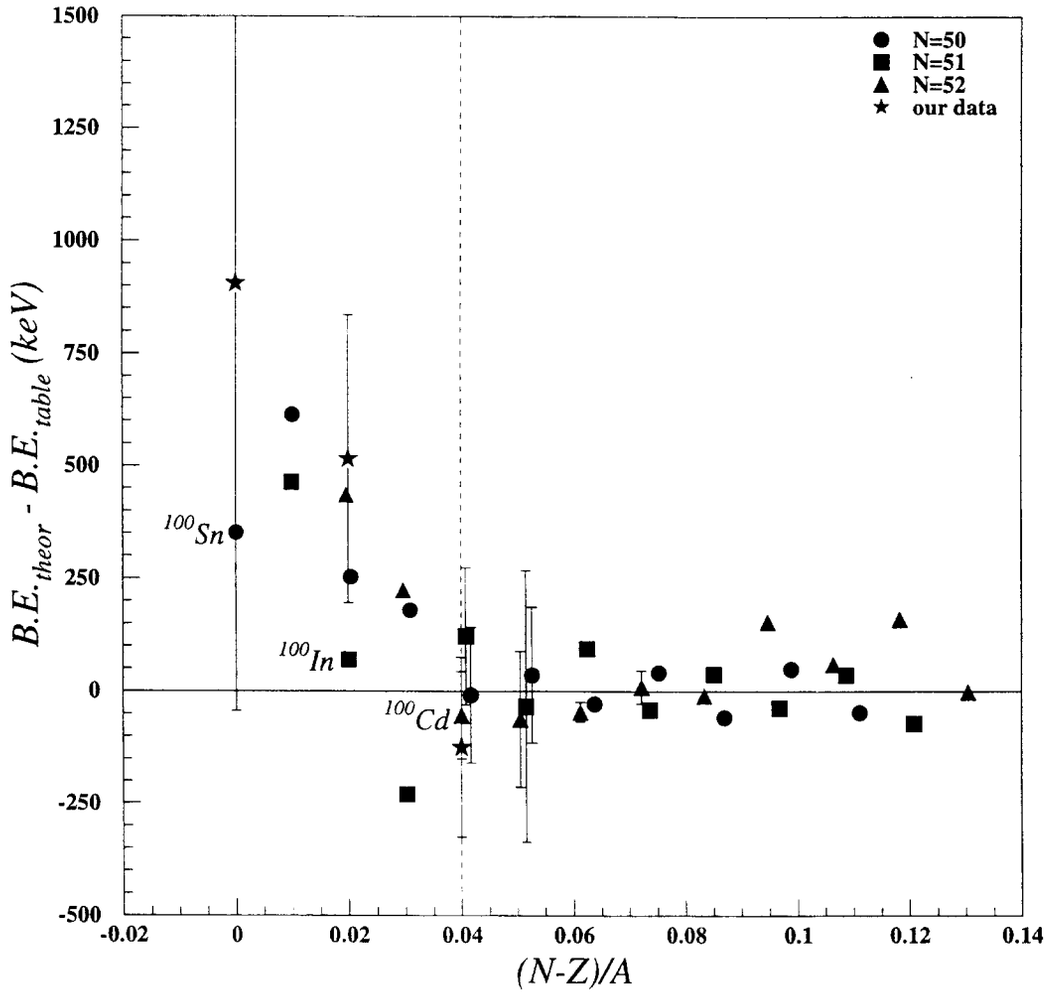

Figure 5: *Comparison between the shell model calculations of Johnstone and Skouras [20] ($B.E._{theor}$) and the mass table of Audi and Wapstra [15] ($B.E._{table}$) for the binding energies of isotones $N = 50$, 51 and 52 from ^{90}Zr to ^{102}Sn. The binding energies of the mass table come either from experimental values (right side of the dashed vertical line) or from systematic trends extrapolations (left side of the line). Our experimental results are represented by black stars.*